Hindawi
Advances in Mathematical Physics
Volume 2021, Article ID 1589182, 11 pages
https://doi.org/10.1155/2021/1589182

Research Article

Application of Image Denoising Method Based on Two-Way Coupling Diffusion Equation in Public Security Forensics

Yiqun Wang,[1,2] **Changpeng He**,[2] **and Zhenjiang Li**[3]

[1]*Key Laboratory of China's Ethnic Languages and Information Technology of Ministry of Education, Northwest Minzu University, Lanzhou 730000, China*
[2]*School of Artificial Intelligence, Gansu University of Political Science and Law, Lanzhou 730070, China*
[3]*School of Cyberspace Security, Gansu University of Political Science and Law, Lanzhou 730070, China*

Correspondence should be addressed to Yiqun Wang; wyq6696@gsupl.edu.cn

Received 11 November 2021; Revised 7 December 2021; Accepted 9 December 2021; Published 30 December 2021

Academic Editor: Miaochao Chen

Copyright © 2021 Yiqun Wang et al. This is an open access article distributed under the Creative Commons Attribution License, which permits unrestricted use, distribution, and reproduction in any medium, provided the original work is properly cited.

This paper uses the web live broadcast and on-demand platform based on the B/S architecture as the application side and designs a video image forensic system that can meet multiple police types and multiple application scenarios. The system uses mobile phones as the video image capture terminal to solve the problem of rapid response and concealment and uses 5G communication technology as the transmission medium to solve the problem of device mobility and link maintenance. The problem of diversification of the use and application modes of multiple police types is solved; the video image evidence is managed in a centralized storage, audit, and export method, and the security and authenticity of the evidence are solved. While the system realizes a series of functions such as the collection, transmission, storage, and application of video image evidence, it also realizes the application-side video image live broadcast function according to actual work needs and solves the large-scale case command and decision-making problem that has been plagued by public security organs. In order to remove the noise in the public security forensic images and to smooth the noise while retaining the details of the image, this paper proposes a denoising algorithm based on the two-way coupling diffusion equation. By improving the second-order partial differential equation, a new diffusion function with better diffusion effect than the original model is constructed. We combined the adaptive edge threshold and stop criterion to establish a new denoising algorithm model, which can get better denoising results. When the noise level is low, the PSNR value and SSIM value of several denoising methods are relatively ideal, and the result is at a higher level, the denoising picture effect is better, and there is no obvious incomplete noise removal or detail problems. As the noise level increases, the denoising results will gradually decrease, and the effects will also vary to different degrees. When the noise intensity increases, visually, it can be clearly seen that the two-way coupled diffusion equation and DnCNN have better denoising effects. When the noise level is high, the two-way coupled diffusion equation network is used to use the clear image and the denoised image for indistinguishable calculation. The method in this paper almost retains all the texture details in the clear image, and there are almost no artifacts and images. On the other hand, the color of the image after denoising by the method in this paper is more vivid, and it is closer to the target picture in terms of picture definition and tone, the denoising effect is ideal, and the generated image has a higher degree of restoration. Compared with the residual GAN, the two-way coupling diffusion equation network converges faster and the network performance is improved.

1. Introduction

The research on the process of obtaining evidence for electronic data in the criminal field has become a hot issue in academic circles. The wide-area and interconnected nature of cyberspace enables cyberbehaviors to act on real spaces thousands of miles away. Therefore, criminal behaviors carried out through the Internet have the characteristics of transregional and transnational borders [1]. In the Internet age, criminal evidence collection of electronic data has become a link that investigators have to face in most cases [2]. For the electronic data and cloud data stored across regions related to the case, evidence collection activities need to rely on remote evidence collection procedures. Remote

electronic data forensics has become a necessary way for electronic data collection in an open network environment. It is different from the traditional investigation and evidence collection modes of personal experience and direct physical contact in criminal proceedings. Electronic data forensics brings to the existing criminal investigation and evidence collection rules [3]. In the era of wide-area interconnection, remote forensics of electronic data stored, transmitted, and processed on remote computers and cloud servers has become an indispensable investigative method. With the further development of distributed data storage, the seizure of the original carrier will become more complicated and inconvenient, and remote forensics that can meet cross-regional requirements will inevitably be more widely used in the future [4].

The volume of public security forensic image data has increased, and how to obtain useful and critical information from it has become more and more important [5]. On the one hand, a lot of data is not all useful to researchers, so when processing big data, preprocessing such as selection or classification must be carried out, otherwise it will increase the difficulty of the data processing process and greatly increase the amount of data storage. On the other hand, the filtered data cannot be used directly. Due to a series of objective reasons such as data transmission, exposure, and storage time, the obtained data will have noise, chromatic dispersion, and other factors that affect the authenticity of the data. There is a big deviation from the real data. In order to obtain accurate information from the image data, removing the noise in the image is the key [6]. However, the public security forensic image is composed of three primary colors (red, green, and blue), which are called R, G, and B three channels. Due to the multichannel characteristics of the public security forensic image, this means that the denoising ratio of the public security forensic image is less than that of the gray image [7]. Compared with grayscale image denoising algorithms, such as denoising methods based on vector representation and denoising methods based on matrix representation, they are not suitable for direct application to public security forensic image denoising [8]. In order to solve the problem of removing noise from public security forensic images, in the subsequent development, researchers proposed a series of denoising algorithms based on tensor representation [9]. With the gradual increase in denoising algorithms for public security forensic images, another problem has arisen [10]. When public security forensic images are contaminated by noise, the channel contains different levels of noise. Nowadays, public security forensic images are widely used in various fields such as surveillance and medical images. Public security forensic image denoising algorithms can play a key role in image restoration and image recognition. Therefore, according to the current problems of removing noise from public security forensic images, it is of great significance to study valuable denoising algorithms.

This article introduces the overall design of a public security video image forensic system based on Android phones. Taking the actual needs of the public security department's current evidence collection work as the starting point and centering on the design policy of "quick response, safe and reliable," the system design goals and overall system architecture are given. It is divided into two parts: mobile forensic terminal and web application terminal. It introduces Android mobile phone video image acquisition, H.264 video image encoding, RTP/UDP protocol encapsulation, application terminal data reception, and video image playback service. This paper analyzes the image denoising algorithm based on partial differential equations, introduces the PM model and TV model, and improves the edge threshold parameter k of the PM model to an adaptive parameter, which reduces the workload of selecting edge threshold parameters for the two-way coupling diffusion equation. In this paper, a two-way coupled diffusion equation network is designed for image denoising, and the results of different denoising methods are compared and analyzed. Noisy pictures under different noise intensity levels are denoised, and no confrontation training is used with others. The noise result also proves the effectiveness of the denoising algorithm in this paper.

2. Related Work

Related scholars put forward the concept of spatial scale and pointed out that solving the heat conduction equation with the original image as the initial value is equivalent to convolving the image and Gaussian function to achieve low-pass filtering [11]. Since the Gaussian filter is isotropically diffused, the edges will be smoothed while denoising, and the details will become blurred. Related scholars have proposed a bilateral filter, which can combine gray levels or colors according to the geometric proximity and photometric similarity of the image and add the spatial distance weight value and the gray information weight value to achieve bilateral filtering [12]. Bilateral filters can eliminate noise well and protect edges at the same time, but the calculation speed is slower. Relevant scholars use Gaussian convolution kernel to filter the image [13]. The filter parameters depend on the signal-to-noise ratio, the mean square error of the noise image, and the value to be repaired.

Robust principal component analysis, matrix completion, and other algorithms can effectively remove the noise in the image, but its main application is to reconstruct and restore the data matrix [14]. Therefore, the problem of image denoising has begun to be a classic of digital image processing. Research topics have received extensive attention [15, 16]. According to the actual characteristics of the image and the true distribution of the frequency spectrum, foreign scholars first proposed that the image is low rank, resulting in a series of classic denoising algorithms, such as dictionary learning and low-rank representation [17]. As an important research route, low-rank representation has a profound impact on image denoising. Unlike RPCA, this method introduces the idea of dictionary learning and constrains low-rank matrices to approximate low rank by constructing a dictionary matrix. In order to make this method more robust to noise and outliers, the observation matrix is usually selected as the dictionary matrix for constraints.

As an extension of grayscale images, public security forensic images have multiple channels. The matrix cannot be accurately represented because the dimension is higher than the matrix, and the tensor can solve this problem. Researchers hope to extend the original matrix denoising framework to public security forensic images and use its model and algorithm to deal with the problem of public security forensic image denoising [18]. This is difficult, because the public security forensic images are three-channel, that is, tensor. The definition of some properties of public security forensic image denoising is still closely related to the matrix, which further shows that matrix-based denoising algorithms can be extended to public security forensic images. At present, for tensors, a major problem that plagues scholars is the inability to accurately define the rank of tensors, which is an NP-hard problem [19]. Therefore, how to remove the noise while maintaining the inherent information of the image and maintaining the stability of its structure has become a major challenge nowadays.

With continuous in-depth research, more and more public security forensic image denoising algorithms have gradually emerged [20]. Many of these algorithms extend the original model to public security forensic images. The color three-dimensional block matching algorithm is a representative algorithm. It first converts the RGB image into a low-dimensional space and then uses a reference three-dimensional block to match each channel. The algorithm performs processing and then aggregates into an image with noise removed. Related scholars have proposed a "noise level function" to evaluate and remove the noise in each channel [21–23]. However, processing each channel separately is much worse than combining the color channels for processing, because this ignores the self-similarity of each channel. Therefore, related scholars have proposed to connect the three signal channels of R, G, and B in a series for denoising, but this does not take into account that the noise level of each noise channel is different, which leads to the appearance of denoising artifacts [24, 25].

3. Method

3.1. Functional Requirements of Video Image Forensic System

3.1.1. Mobile Phone Collection Terminal. According to the work focus and existing shortcomings of the seven work scenarios of video image forensics of public security organs, as well as the actual needs of video image forensic business, the main functions of the public security video image forensic system based on android mobile phones are designed.

In order to meet the needs of public security organs for quick response, portability, flexibility, safety, and concealment of evidence collection, the system's video image capture terminal is developed using a smart phone based on the Android system. While ensuring the core requirements of the video image capture terminal such as clear captured images and stable and reliable network transmission, it also highlights compatibility, ease of use, and reliability on the basis of existing smart phone hardware devices and mobile phone networks. This article proposes the following specific functional requirements for the mobile phone collection terminal of the video image forensic system.

The forensic officer opens the forensic software in the mobile phone, enters the account and password of the collection device, and activates the mobile phone collection terminal. During this process, the mobile phone collection terminal will communicate with the application terminal to verify the entered account password and at the same time verify whether the mobile phone IMEI code of the collection terminal is in the device list. When the verification is passed, the collection terminal is active, and video image forensics and video image live broadcast can be performed at any time. At the same time, the device and its location information will appear in the online device list on the application side.

The system provides video image capture setting options, which can set the resolution, frame rate, bit rate, etc. of the captured video image. At the same time, it also provides a selection of scene modes, including normal mode, tracking mode, low light mode, video image quality priority mode, and network transmission priority mode.

3.1.2. Business Application Side. In order to meet the needs of the public security organs for video image forensics and command and decision-making during major mass incidents, major cases, and disaster relief, the business application of the video image forensic system is set up on the Internet and can automatically receive video images from the mobile phone collection terminal. Various applications for evidence video images are provided according to the actual needs of the public security organs.

The system user uses a browser to connect to the business application and enters the account password to log in. After users log in to the system, they can perform video and image live broadcast, on-demand broadcasting, sorting, exporting, and other applications. The functions that can be used vary according to the department and role of the account. The business application terminal automatically receives the live video images and forensic video images sent back by the mobile phone collection terminal in the online list.

The data receiving module submits the data to the transcoding storage function while receiving the data from the mobile phone. It first analyzes and restores the communication protocol and then reencodes the data video image to generate a video image format suitable for network playback and easy to store. If the live video image is received, the live stream is generated and provided to the video image live broadcast module at the same time. Finally, the received complete video image data is named and stored in the designated location according to the rules. The system automatically backs up all evidence video images on a regular basis.

Based on the GIS platform, there are mainly two ways of display. One is the display of the location of the online collection terminal. The location of the current online collection terminal equipment is displayed on the GIS map, which is convenient for the commander to conduct on-site command and issue tasks according to the location of each

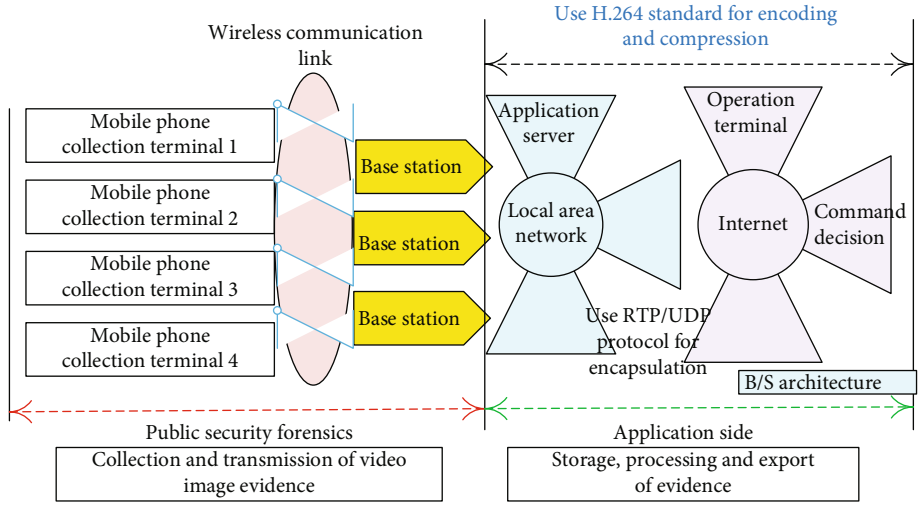

Figure 1: System structure design diagram.

investigator. The second is the presentation of evidence video images. Since the geographic location is collected every time the video image is collected for evidence, all systems can mark the collection location of each piece of video image evidence on the GIS platform, which is convenient for the investigators to organize and apply the video image of the evidence.

3.2. The Overall Framework Design of the Video Image Forensic System. By summarizing the design of the system function and the requirements of public security video image forensics in the previous section, this article divides the video image forensic work of the public security department into two parts: forensics and application. Forensics refers to the collection and transmission of video image evidence, while application refers to the storage, processing, and export of evidence. By organizing and summarizing the key tasks of each scene of video image forensics, the structure of the public security video image forensic system based on Android mobile phones is designed, as shown in Figure 1.

In Figure 1, the entire public security video image forensic system can be roughly divided into left and right parts. On the left is the wireless communication link based on the Android mobile phone acquisition terminal and the mobile phone's 5G network, which mainly completes the functions of forensics and return. The mobile phone application encodes and compresses the collected original video image data using the H.264 standard and then encapsulates the encoded video image frames using the RTP/UDP protocol. The encapsulated data enters the Internet through the base station and the operator's gateway through the mobile phone network built by the mobile communication operator. In this part, the mobile phone network is constructed and maintained by the operator, and the video image forensic system only needs to complete the design and implementation of the video image collection terminal. The right part of Figure 1 is the application part of the system, which is built on the Internet. The server receives the video image data sent from the mobile phone collection terminal and then performs protocol analysis and video image transcoding. The final data obtained generates the live stream while transferring the video image data to the server. The user terminal uses a browser to log in to the application terminal and can watch the live broadcast or on-demand historical video images in the server. This part is based on the B/S architecture, and the client is implemented based on a browser, and no development is required. It is necessary to build a server based on video image reception, decoding, and playback.

It can be seen from the system structure diagram that the typical workflow of video image forensics is to collect video images on the collecting terminal after login verification and then perform video image coding compression and protocol encapsulation while collecting. Then, the video image data is transmitted to the application terminal through the transmission link, and after the application terminal receives it, it is restored and encoded through the protocol, and the video image is stored in the file server. The video image analysis and investigation log in to the application-side system to play and view the video image evidence. In this typical working scenario, the working sequence diagram among the collection terminal, the application terminal, and the user is shown in Figure 2.

3.3. Mobile Phone Collection Terminal Solution. Obtaining video image data through the Android system can be achieved by using the API interface provided by the Android SDK. In Android 2.0 and subsequent versions, the Camera class and MediaRecorder class provided by the system can be used to capture video image data from the camera. Among them, the MediaRecorder class mainly implements the playback of audio, video images, and other media. To use it to capture camera data, you need to save the captured video image data locally and then process it. There are two problems with this process. One is that confidentiality will be poor, and the other is that the process is cumbersome and complex and the data is poor in real-time. The camera

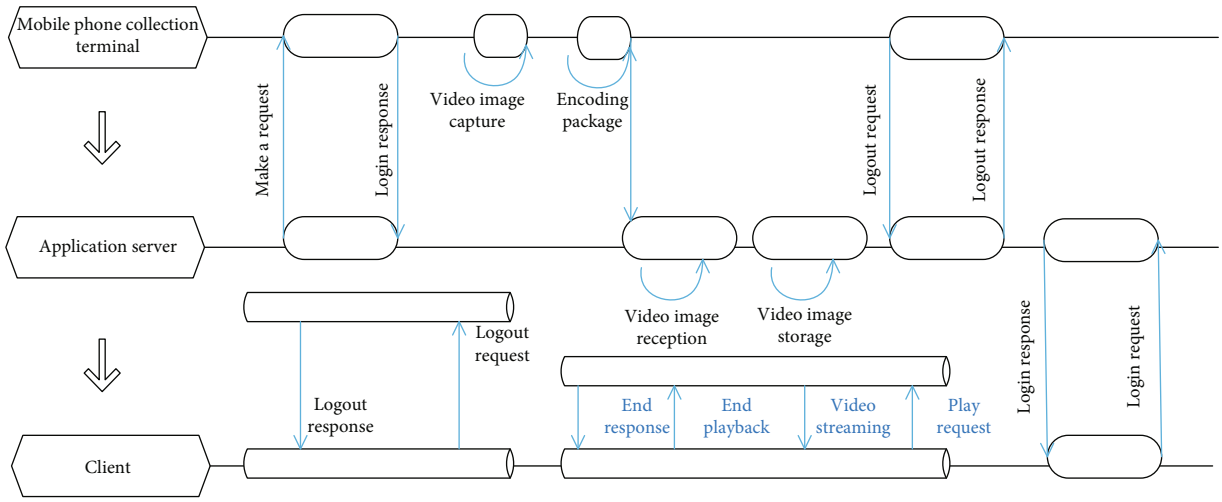

Figure 2: System sequence diagram.

class mainly implements the access to the mobile phone camera and captures the video image data of the preview frame while previewing the video image. Comparing the two methods, this article uses the camera class to achieve the capture of the original video image data.

The mobile phone acquisition terminal of the video image forensic system studied in this paper is not developed for a single type of mobile phone hardware. Instead, based on actual use requirements such as rapid response and concealment, the system encourages the hardware diversity of the mobile phone acquisition terminal. In this case, the workload and difficulty of developing hardware coding for various brands and models of mobile phone hardware are large and difficult. This paper adopts the scheme of transplanting the open source H.264 encoder into the Android system for soft coding.

If the size of the IP packet is smaller than the current network MTU, then the IP packet can be directly transmitted on the link. If the IP packet is greater than the MTU value of the current network, the IP packet will be divided into multiple IP packets during transmission, and each packet will be less than the MTU value. Therefore, the closer the IP packet size is to the current network MTU value, the higher the network transmission efficiency. IP packets have a smaller MTU value, and more IP packets need to be sent to send the same data. On the contrary, not only will each IP packet be split when it is sent, making the actual number of packets sent more, and packet loss will inevitably occur in actual transmission. Assuming that a data packet larger than the MTU value is split into multiple small IP packets, one of which is lost during transmission, it cannot be combined into the original large IP packet at the receiving end, which will cause the entire large IP packet to be retransmitted. Therefore, in network transmission, the current network MTU value should be clarified, and the actual IP packet size should be as close as possible to the MTU value to improve network transmission efficiency.

This article believes that the key to RTP protocol encapsulation is that the size of the encoded data frame to be sent should be appropriate, and it cannot be greater than the current network MTU value minus the size of 3 headers (i.e., 40 bytes).

3.4. Application-Side Solution. The main function of the application terminal of the public security video image forensic system is to receive the video image evidence returned by the mobile phone collection terminal and restore the communication protocol and H.264 encoding. While providing video image live streaming, it saves video image data and provides on-demand services and provides management functions and export functions for video image evidence according to the actual needs of public security work.

The data receiving and storage module is a key part of the application side of the video image forensic system. It acts as a bridge linking the mobile phone collection side and the application side in the system and is responsible for communication with the collection side, video image data reception, communication protocol restoration, and video image decoding. A series of functions such as live stream generation and video image data storage are the basis of various video image forensics and decision-making command functions on the application side.

The function of exporting evidence requires cooperation between users of investigation and case handling and users of legal supervision. The investigating and handling user is responsible for the first half of the process. From the perspective of public security business, the video image data returned by the collection terminal is screened, and the video image that can be used as evidence is found for submission. The MD5 code of the selected video image must be verified before drawing or video image interception to ensure that the video image data is authentic and reliable. After the submission is successful, the latter half of the process needs to be completed by law enforcement and supervision of users. The law enforcement supervision user reviews the evidence export and submits it and executes the export

after it is correct. Finally, the video image evidence and the list of evidence generated by the system are handed over to the investigator who submitted it for export.

3.5. Two-Way Coupling Diffusion Equation. Gaussian filtering is a linear smoothing filter, which is a widely used image denoising algorithm. The principle of the Gaussian filter is to convolve the image and the Gaussian kernel and filter in this way:

$$u_\sigma(x,y) = G_\sigma \nabla u(-x,y). \tag{1}$$

The convolution kernel is

$$G_\sigma = \frac{1}{2\pi}\sigma^{-2}e^{-2\sigma\bullet\left(x^2+y^2\right)}. \tag{2}$$

 is the variance of the Gaussian function. The variance is different, the size of the convolution kernel is different, and the smoothness of the image is also different.

Solve the heat conduction equation with the original image (x, y) as the initial value is equivalent to convolving the image with the Gaussian function. The heat conduction equation can be expressed as

$$\frac{\partial u}{\partial t} = (c-1)\left(\frac{\partial u}{\partial x} + \frac{\partial u}{\partial y}\right). \tag{3}$$

Among them, the thermal conductivity c is a constant, and the parameter $б$ of the Gaussian filter is proportional to the time parameter t of the equation solution.

Since the diffusion coefficient c of the heat conduction equation is constant, the diffusion function has the same diffusion speed in the direction of 360° during the filtering process, so it is an isotropic diffusion method. Many important geometric features in the image, such as details of edges and textures, become relatively smooth in the process of isotropic diffusion (i.e., denoising).

The second-order nonlinear diffusion equation based on PDE is an anisotropic diffusion equation:

$$\begin{aligned} \frac{\partial I(x,-y,-t)}{\partial t} &= \operatorname{div}\left[c(\nabla I)|\nabla I|\right], \\ I(x,y,0) &= I_0(x,-y). \end{aligned} \tag{4}$$

Two typical spread functions are given using Cauchy's law and Gauss's law:

$$\begin{aligned} c_1(\nabla I) &= \frac{k^2 + k\nabla I}{k^2 - \nabla I^2}, \\ c_2(\nabla I) &= e^{-(\nabla I/k)^2}. \end{aligned} \tag{5}$$

In the formula, k is the edge threshold parameter, which is a constant selected by humans to control the degree of diffusion.

The parameter k determines the smoothness of the resulting image. When the value of k is too small, the noise in the image still exists. On the contrary, when the k value is set to a large value, the image will be excessively smoothed, and edge and detail information will be lost. The appropriate value of k is usually selected based on experience and experimentation, which requires experienced testers or requires a large number of experiments to determine the value of k, which increases a lot of work. Therefore, it is necessary to propose an adaptive selection strategy in the diffusion coefficient.

In the iterative process, the calculation of the value of k is added. When the pixel value of the denoising image changes with the number of iterations, the edge threshold parameter k also changes accordingly, as shown in the following formula:

$$k = \frac{\prod_{ij=-1}^{t}\left(I_{ij}\sigma\right)\left|I_{ij}\right|}{mn}(m+n). \tag{6}$$

The total variation model is as follows:

$$J_\lambda(u) = \int_{E\cup D}(\nabla u)^2 dxdy - (u - \lambda u_0)^2. \tag{7}$$

Among them, the first term is a regular term, and its function is to find the optimal solution in the total variation of the image in the $E \cup D$ region. The second item is the data fidelity item, which can smooth the area to be repaired. u is the reference image, u_0 is the image to be repaired, and λ is the regularization parameter, used to balance the weight of the regular item and the data item.

The gradient descent equation of the energy functional is

$$\lambda_e(u - u_0) - \operatorname{div}\left(\frac{2\nabla u}{|\nabla u|}\right) = 0. \tag{8}$$

In it,

$$\lambda_e = \begin{cases} -\lambda & x \longrightarrow E, \\ 1 & x \longrightarrow D. \end{cases} \tag{9}$$

The discretization of the total variation model is

$$\prod_{X\longrightarrow B}(\nabla u_x)^{-1}|u_X - u_0| - \lambda u_0 = 0. \tag{10}$$

The final expression is

$$u_0 = \prod_{X\longrightarrow B} u_X \nabla u_x - \frac{(1+\lambda)u}{\nabla u_x}. \tag{11}$$

3.6. Image Quality Evaluation Method. Mean square error (MSE) and peak signal-to-noise ratio (PSNR) are the two most basic and most commonly used full-reference image quality evaluation methods. The method is relatively simple, and the calculation is relatively easy. The definition of the mean square error method is to calculate the average of the sum of squares of the pixel difference between the original image and the distorted image, that is, the average of the

error sum of squares, and use this as a standard to judge the degree of distortion of the image.

$$\mathrm{MSE} = \left(\frac{1}{m} + \frac{1}{n}\right) \prod_{i=0}^{m-1} \prod_{j=0}^{n-1} \left| f_{ij} - f'_{ij} \right|. \tag{12}$$

Among them, m and n are the length and width of the image, f_{ij} represents the pixel value of the original image, and represents the pixel value of the distorted image.

The peak signal-to-noise ratio is calculated using the ratio of the maximum signal amount to the noise intensity. Since a digital image is composed of dot pixels one by one, expressed in discrete digital form, the maximum pixel value of the image is used to replace the peak value of the signal:

$$\mathrm{PSNR} = 10 \lg \left(L^2 \mathrm{MSE}\right). \tag{13}$$

Among them, L is the maximum gray value of the image, and the range of gray value is generally from 0 to 255, so L usually takes 255. The unit of PSNR is dB. Generally speaking, the larger the value, the higher the image quality and the smaller the distortion.

A measurable deviation between statistical regularities can be observed from natural images. This method only uses this deviation and does not need to use artificially degraded images for training. Therefore, it does not require the original undegraded image, and the image quality can be evaluated without understanding the expected distortion or the judgment of the human eye on the image. First, the method constructs a set of "quality awareness" features and fits it to a multivariate Gaussian (MVG) model. The quality perception function is derived from a simple but highly regular natural scene statistics (NSS) model. Then, the quality of a given test image is expressed as the distance between the multivariate Gaussian (MVG) fitting of the NSS features extracted from the test image and the MVG model of the quality perception features extracted from the natural image corpus, as shown in the following formula:

$$D(v_1, v_2) = \left[(v_1 - 2v_2)^T \cdot (v_1 - 2v_2) \right]^{1/2}. \tag{14}$$

Among them, v_1 and v_2 are the mean vector of the natural MVG model and the MVG model of the distorted image, respectively.

4. Results and Discussion

4.1. Network Training Experiment. In this experiment, this article uses the RMSprop optimizer for pretraining and sets the hyperparameter of the optimizer to $\alpha = 1 * 10 - 5$. At the same time, use a network with the same learning rate as in the pretraining process, and set the batch size to 10. TensorFlow using the Windows 10-64 bit operating system is used to build the network in the Python 3.5 environment. The model proposed in this article is trained and tested on an Inter(R) Core(TM) i7-6700K CPU with a total memory of 16 G.

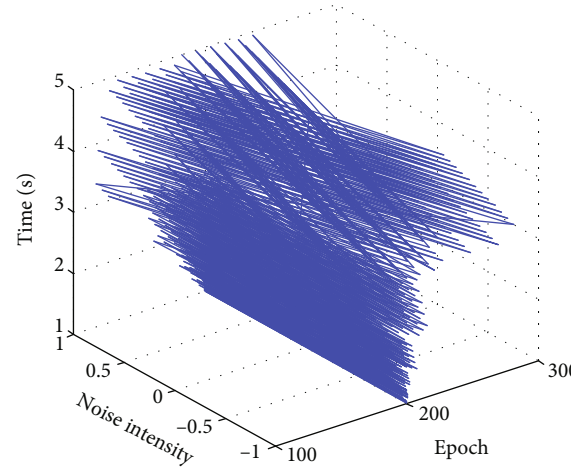

Figure 3: Training time for 300 epochs.

According to the experimental results, the two-way coupled diffusion equation network exhibits superior denoising effects. On the one hand, the improved network structure makes the image texture details and colors more outstanding. On the other hand, the added VGG perceptual loss can better guide the network training. We compare the experimental results of the images generated during the training process. Figure 3 shows the training time of the original network model in 300 epochs.

4.2. Comparison Experiment of PSNR Value and SSIM Value. This article uses a data set of 3000 images with different noises for training. Considering three noise levels, namely, 15, 25, and 50, the WGAN of this article is trained and optimized by removing the Gaussian noise of noisy images with known noise levels. In this paper, the training data set is cropped at intervals of 10, and the color block size is set as the crop patch for model training. For the test images, two different test data sets are used for comprehensive evaluation. One test data set is the BSD68 data set, and the other contains 8 Gaussian images that are widely used to evaluate denoising methods. At the same time, through data expansion, the amount of experimental data in this paper is sufficient to obtain a powerful noise reduction effect.

For noise reduction results, four methods are compared, including two nonlocal optimization methods (CBM3D and EPLL) and two deep learning methods (TNRD and DnCNN). It is used to quantitatively evaluate the denoising effect and comprehensively evaluate the denoising effect in combination with subjective visual perception. The results of image denoising are shown in Figures 4 and 5. Figure 4 shows the peak signal-to-noise ratio (PSNR) of each method, and Figure 5 shows the structural similarity (SSIM) of each method under different noise intensities. It can be seen that the PSNR value and SSIM value of the method in this paper are higher than those of the other two algorithms. In this paper, the two-way coupled diffusion equation network combines deep multiscale feature extraction and deep jump residual network multilayer feature extraction, and the image denoising effect obtained is better than expected results.

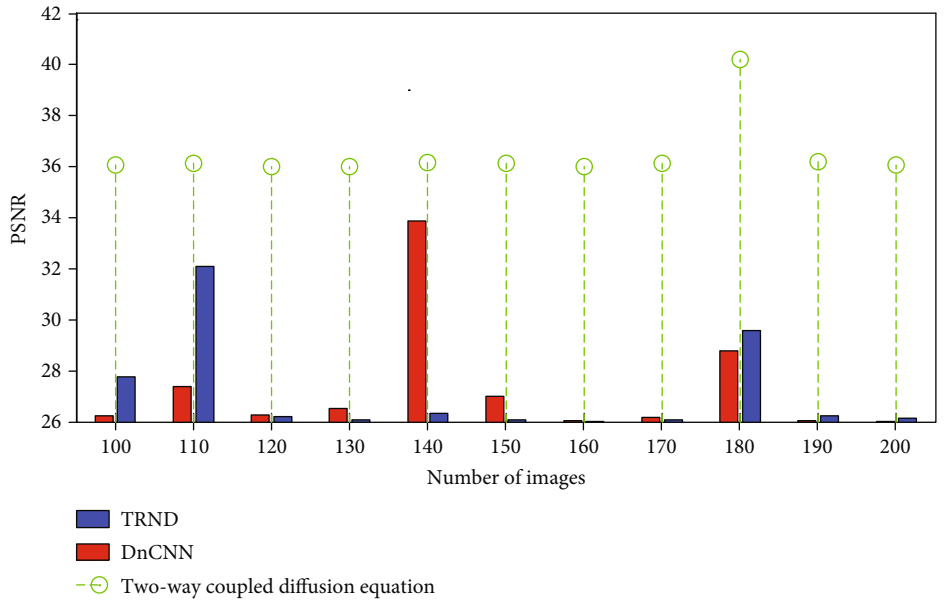

Figure 4: PSNR values of different image denoising methods.

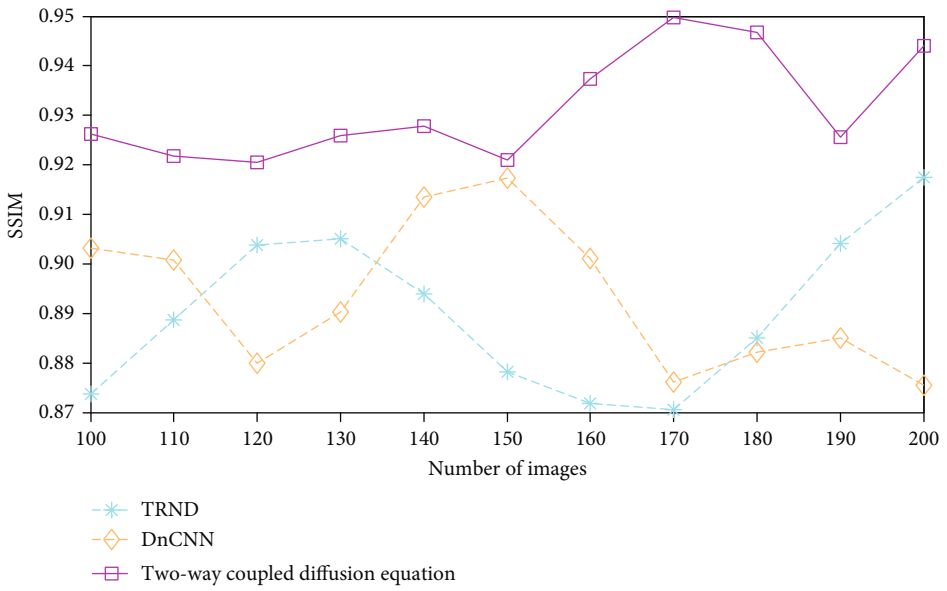

Figure 5: SSIM values of different image denoising methods.

It can be seen from Figure 5 that different denoising methods have differences in the denoising results of each image. DnCNN tends to produce smoother texture details, which is not very good for image edge processing. TNRD can restore better texture details and edge features, but the denoising image has poor smoothness and the effect is not very satisfactory. The method in this paper is superior in texture details and smoothness, and the visual effect is better.

The two-way coupled diffusion equation is superior to other denoising methods in most denoising results. Because in images with repetitive structure, the processing result based on the self-similarity prior is better than discriminative learning. If the image has fewer nonlocal self-similar blocks, the performance of this method is better. Therefore, the two-way coupling diffusion equation can obtain better denoising effect by using better network structure and loss function. The results show that the two-way coupling diffusion equation has better performance for image denoising under high noise levels.

The method in this paper makes full use of multiscale features through deep convolution, avoids feature blur, reduces the loss of useful features, uses jump connections between noise features and extracted noise to generate denoising features, and uses block jump connections between to mix high-level features and low-level features. Compared with several other methods, the method in this paper achieves the effect of precise denoising. Combined with the results of denoising, it can be seen that the noise

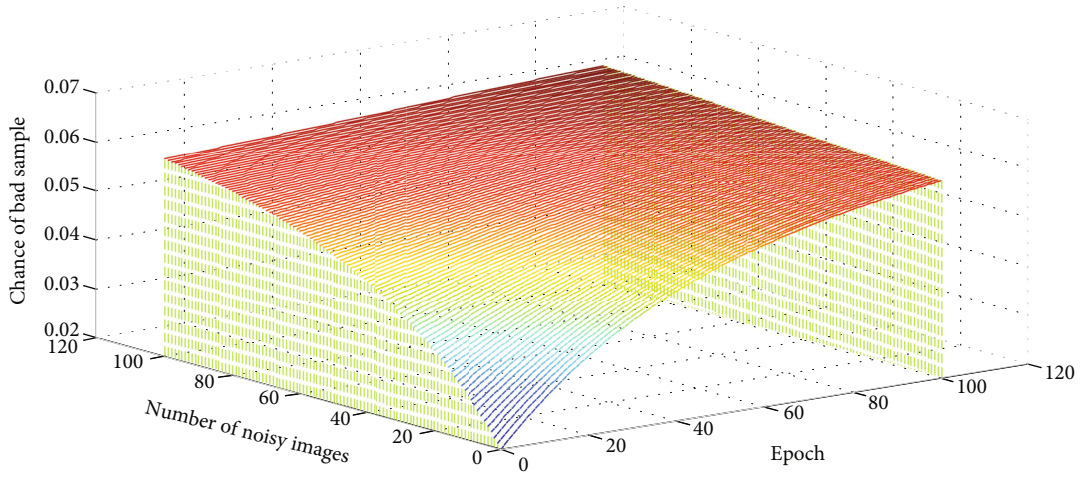

Figure 6: Changes in the denoising image of the two-way coupling diffusion equation.

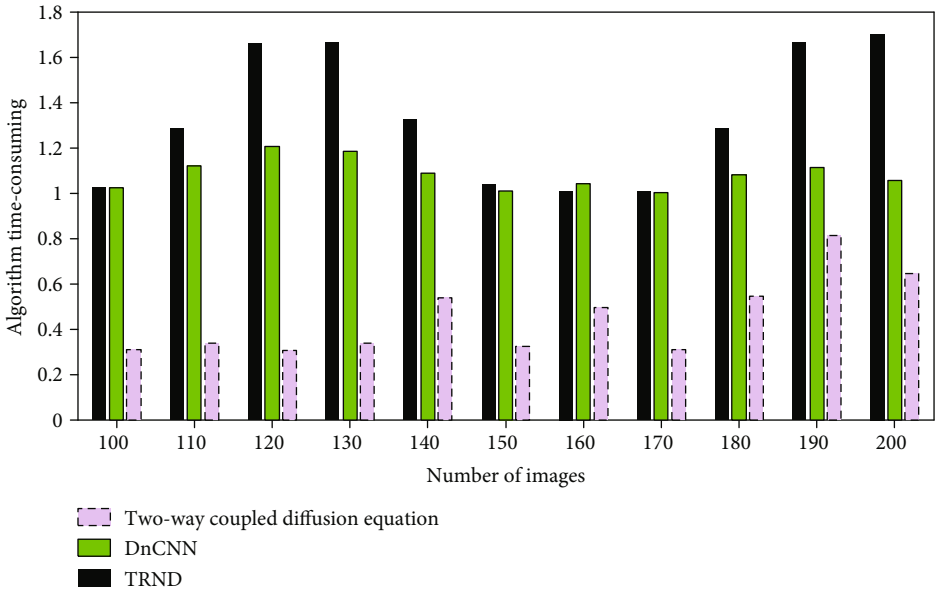

Figure 7: Time-consuming comparison of different algorithms.

level is directly related to the denoising effect. When the method in this paper denoises low-noise images, the denoising results processed by the two-way coupling diffusion equation can better retain the texture details of the image, indicating that the network is in the case of low-intensity noise and high-intensity noise interference. Both can learn the detailed features of the image better and retain the color and contrast of the denoised image during feature reconstruction.

The above experimental results show that the algorithm in this paper can also restore image details well in the case of high-intensity noise. When the network performs different levels of feature extraction, due to the interference of high-intensity noise, the extracted noise is quite different from the actual one, but under the correction of the loss function, the visual effect of the denoised image is better.

The change of PSNR value of the denoised image is shown in Figure 6. It can be seen from the figure that the discriminator training process of the two-way coupled diffusion equation denoising method is stable, and the network training efficiency is significantly improved, the probability of bad samples is greatly reduced, and the performance of the denoising network is effectively improved.

The experiment selects multiple test images from the standard image library and estimates the average running time of the algorithm based on the above-mentioned experimental platform. The results are shown in Figure 7. Because of the time-consuming conventional feature extraction operation, the model efficiency is low, and the running time of the three algorithms is close. However, the two-way coupled diffusion equation network takes a shorter time than other algorithms.

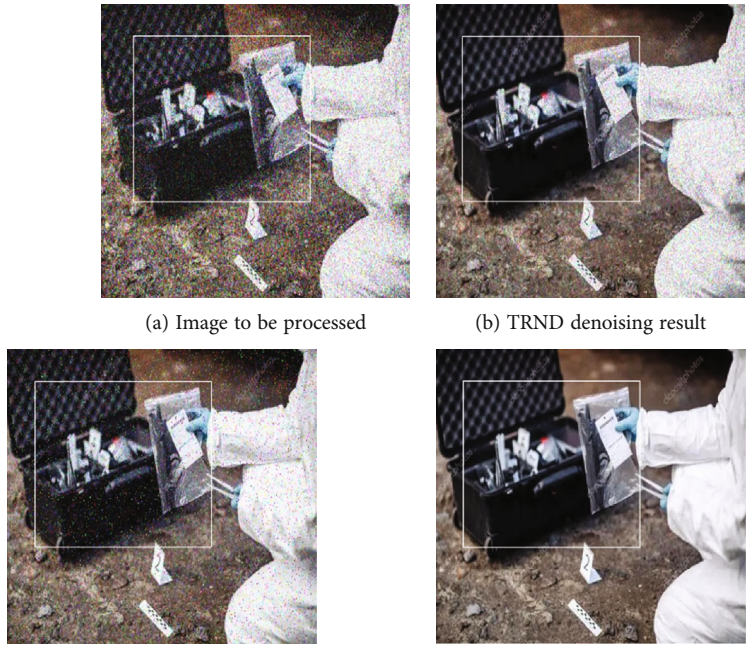

(a) Image to be processed (b) TRND denoising result

(c) DnCNN denoising result (d) Two-way coupling diffusion equation denoising result

Figure 8: Denoising results of complex background images for public security forensics.

4.3. Testing of Complex Background Images for Public Security Forensics. We create a data set of 1000 public security forensic complex background images to train the network and a test set of 10 images. When processing general natural images, tiny details have little effect on the subsequent research and application of denoising images. In the public security forensic image processing, the impact of tiny information on the image cannot be ignored. In high-precision diagnosis, any small mistakes will lead to irreparable consequences. At this time, the requirements for image denoising are very harsh, and it is necessary to complete the denoising task while retaining as much small information as possible.

Before the image data set is input to the network for denoising, in order to reduce the network training time, the image is cropped to a size of $256 * 256$. In the test image set, the image size is set to $397 * 397$. At the same time, the complex background image of public security forensics is processed. The process is also obtained by adding noise. The complex background image processing of public security forensics is complicated, and the data set is limited. We show an example of the denoising results of the complex background image of public security forensics, as shown in Figure 8. It can be seen that the two-way coupling diffusion equation has the best denoising effect.

5. Conclusion

The system uses mobile phones as the video image acquisition terminal to solve the problems of rapid response and concealment and uses the mobile phone communication network as the transmission medium to solve the problems of device mobility and link maintenance. The problem of diversification of the use and application modes of multiple police types is solved; the evidence obtained is managed by centralized storage and auditing and export; the security and authenticity of the traditional evidence collection method are solved. Under the premise of achieving a series of functions for the collection, transmission, storage, and application of video image evidence, the system realizes the application-side video image live broadcast function according to the actual public security work requirements and solves the large-scale cases (incidents) that have been plagued by public security organs. In order to verify the effect of the image denoising method in this paper, PSNR and SSIM are used as image quality evaluation indicators. After comparing the method proposed in this article with several traditional image denoising methods, we can see that the method proposed in this article has improved both the PSNR value and the SSIM value, especially the results of image denoising using the two-way coupled diffusion equation method. From the above point of view, the image denoising effect obtained by the method proposed in this paper is better than the result of combining the DCGAN. From the perspective of subjective vision, the restored image has better clarity and authenticity. Therefore, the method proposed in this paper has good practicability in realizing the research of image denoising. Due to the time and the lack of computer hardware conditions, the method proposed in this paper takes a long time to train the network and is insufficient for the training of the network, which leaves a lot of room for improvement in the denoising results. When the hardware meets the standard, the two-way coupling diffusion equation network proposed in this paper can obtain a more adequate training effect. Since it is time-consuming to generate a denoising network, this paper cannot achieve the

optimal value of the parameters through precise adjustment of the parameters in a limited time. Therefore, this paper is based on the proposed improved network to obtain the best denoising result at this time. At the same time, the ideal number of iterations can be sought to achieve the optimal solution, thereby improving the efficiency of network training, which can become a follow-up research direction.

Data Availability

The data used to support the findings of this study are available from the corresponding author upon request.

Conflicts of Interest

The authors declare that they have no known competing financial interests or personal relationships that could have appeared to influence the work reported in this paper.

Acknowledgments

This work is supported by the innovation ability improvement project of colleges and universities in Gansu Province (No. 2020B-164), the Natural Science Foundation of Gansu Province (20JR10RA335), the scientific research projects of Gansu University of Political Science and Law (No. 2017XQNLW04, No. GZFXQNLW003), the Innovation and Entrepreneurship Project of Gansu Province in 2021, Gansu University of Political Science and Law Judicial Appraisal Center research fund (No. jdzxyb2018-09), and also Innovation and Entrepreneurship Training Program of Gansu University of Political Science and Law (No. X202011406011).

References

[1] S. Patil and S. Sheelvant, "Survey on image quality assessment techniques," *International Journal of Science and Research*, vol. 4, no. 7, pp. 1756–1759, 2015.

[2] W. He, H. Zhang, L. Zhang, and H. Shen, "Total-variation-regularized low-rank matrix factorization for hyperspectral image restoration," *IEEE Transactions on Geoscience and Remote Sensing*, vol. 54, no. 1, pp. 178–188, 2016.

[3] X. Liu and L. Huang, "A new nonlocal total variation regularization algorithm for image denoising," *Mathematics and Computers in Simulation*, vol. 97, pp. 224–233, 2014.

[4] D. Bresch-Pietri and M. Krstic, "Delay-adaptive control for nonlinear systems," *IEEE Transactions on Automatic Control*, vol. 59, no. 5, pp. 1203–1218, 2014.

[5] A. Fell, "A free and fast three-dimensional/two-dimensional solar cell simulator featuring conductive boundary and quasi-neutrality approximations," *IEEE Transactions on Electron Devices*, vol. 60, no. 2, pp. 733–738, 2013.

[6] M. E. Kiziroglou, S. W. Wright, T. T. Toh, P. D. Mitcheson, T. Becker, and E. M. Yeatman, "Design and fabrication of heat storage thermoelectric harvesting devices," *IEEE Transactions on Industrial Electronics*, vol. 61, no. 1, pp. 302–309, 2014.

[7] K. Ma, W. Liu, T. Liu, Z. Wang, and D. Tao, "dipIQ: blind image quality assessment by learning-to-rank discriminable image pairs," *IEEE Transactions on Image Processing*, vol. 26, no. 8, pp. 3951–3964, 2017.

[8] Y. Chang, L. Yan, H. Fang, and C. Luo, "Anisotropic spectral-spatial total variation model for multispectral remote sensing image destriping," *IEEE Transactions on Image Processing*, vol. 24, no. 6, pp. 1852–1866, 2015.

[9] V. Estellers, S. Soatto, and X. Bresson, "Adaptive regularization with the structure tensor," *IEEE Transactions on Image Processing*, vol. 24, no. 6, pp. 1777–1790, 2015.

[10] D. Bresch-Pietri, C. Prieur, and E. Trélat, "New formulation of predictors for finite-dimensional linear control systems with input delay," *Systems and Control Letters*, vol. 113, pp. 9–16, 2018.

[11] P. A. Basore, "Efficient computation of multidimensional Lambertian optical absorption," *IEEE Journal of Photovoltaics*, vol. 9, no. 1, pp. 106–111, 2019.

[12] T. Yokota, Y. Inoue, Y. Terakawa et al., "Ultraflexible large-area physiological temperature sensors for multipoint measurements," *Proceedings of the National Academy of Sciences of the United States of America*, vol. 112, no. 47, pp. 14533–14538, 2015.

[13] Wu Cheng and K. Hirakawa, "Minimum risk wavelet shrinkage operator for Poisson image denoising," *IEEE Transactions on Image Processing*, vol. 24, no. 5, pp. 1660–1671, 2015.

[14] J. Xu, L. Zhang, and D. Zhang, "External prior guided internal prior learning for real-world noisy image denoising," *IEEE Transactions on Image Processing*, vol. 27, no. 6, pp. 2996–3010, 2018.

[15] H. Wu and S. Yan, "Computing invariants of Tchebichef moments for shape based image retrieval," *Neurocomputing*, vol. 215, pp. 110–117, 2016.

[16] G. Chen, Y. Wang, W. Pi et al., "Heat leakage analysis on Peltier current leads of different structures," *IEEE Transactions on Applied Superconductivity*, vol. 26, no. 7, pp. 1–4, 2016.

[17] M. Rakhshanfar and M. A. Amer, "Sparsity-based no-reference image quality assessment for automatic denoising," *Signal, Image and Video Processing*, vol. 12, no. 4, pp. 739–747, 2018.

[18] M. Lebrun, M. Colom, and J.-M. Morel, "Multiscale image blind denoising," *IEEE Transactions on Image Processing*, vol. 24, no. 10, pp. 3149–3161, 2015.

[19] H. Cheng and S. M. Chung, "Orthogonal moment-based descriptors for pose shape query on 3D point cloud patches," *Pattern Recognition*, vol. 52, pp. 397–409, 2016.

[20] H. Shoji, J. Uruno, M. Isogai, and T. Yanagidaira, "All-metals induction heating system with switching between full-bridge and half-bridge inverter configurations," *IEEJ Journal of Industry Applications*, vol. 5, no. 3, pp. 289–295, 2016.

[21] J. Zhang and K. Hirakawa, "Improved denoising via Poisson mixture modeling of image sensor noise," *IEEE Transactions on Image Processing*, vol. 26, no. 4, pp. 1565–1578, 2017.

[22] Y. Chen, X. Cao, Q. Zhao, D. Meng, and Z. Xu, "Denoising hyperspectral image with non-i.i.d. noise structure," *IEEE Transactions on Cybernetics*, vol. 48, no. 3, pp. 1054–1066, 2018.

[23] H. Zhu, Y. Yang, Z. Gui, Y. Zhu, and Z. Chen, "Image analysis by generalized Chebyshev-Fourier and generalized pseudo-Jacobi- Fourier moments," *Pattern Recognition*, vol. 51, pp. 1–11, 2016.

[24] Y. Osawa, H. Morimitsu, and S. Katsura, "Control of thermal conductance with detection of single contacting part for rendering thermal sensation," *IEEJ Journal of Industry Applications*, vol. 5, no. 2, pp. 101–107, 2016.

[25] K. Zhang, W. Zuo, and L. Zhang, "FFDNET: toward a fast and flexible solution for CNN-based image denoising," *IEEE Transactions on Image Processing*, vol. 27, no. 9, pp. 4608–4622, 2018.